Flux-Lattice Melting in Amorphous Composite In/InO_x Two-Dimensional Superconductors

P. L. Gammel, A. F. Hebard, and D. J. Bishop
AT&T Bell Laboratories, Murray Hill, New Jersey 07974
(Received 15 October 1987)

We report the phase diagram for magnetic fluxoids in two-dimensional In/InO_x superconducting films. The films are sputtered directly onto high-Q silicon oscillators. The melting of the vortex lattice is signaled by a peak in the attenuation and a shift of the resonant frequency of the oscillator, caused by the rapid change in mobility of the vortex array. The zero-field limit of the melting temperature can be fitted by the Kosterlitz-Thouless model. However, the magnetic field dependences disagree with the current theoretical picture.

PACS numbers: 74.60. Ge, 74.75.+t

With the applied field between H_{c1} and H_{c2} a type-II superconductor is permeated by an array of flux lines, each carrying one quantum of flux. Abrikosov[1] was the first to predict that these would form into a triangular lattice. Such lattices have been imaged with high-resolution Bitter-pattern techniques[2] and neutron scattering.[3] This lattice behaves as a solid with a well-defined shear modulus[4] at low temperatures and fields. In superconducting films in which the vortices are effectively two dimensional this solid undergoes a melting transition below the resistive transition temperature, T_c. It has been predicted[5,6] that this melting should be a Kosterlitz-Thouless (KT) type melting, mediated by the unbinding of dislocation pairs. Measurements on granular aluminum films have shown a vortex mobility transition consistent with such behavior.[7]

In this Letter we report mechanical measurements of flux-lattice melting and present the phase diagram as a function of temperature and magnetic field for the flux lattice in amorphous composite In/InO_x films. The observed phase diagram is qualitatively similar to the theoretical form, but has important quantitative differences. While the previously published theory[5] predicts no field dependence to the melting temperature in the intermediate-field regime, we see a linear dependence. Inclusion of H/H_{c2} correction would improve the qualitative agreement in the shape of the phase diagram.[8] The theory also predicts that the melting line should approach H_{c2} at low temperatures, while the measured line remains substantially below this value. The theory has one parameter, A_1, which may be used to fit the zero-field limit of the melting temperature, T_M. While A_1 can in principle be calculated, at present it has only been estimated. Our fitted value lies well within the estimate for a KT-type melting.

The experimental setup used in these experiments is shown schematically in the inset of Fig. 1. The basis of the experiment is a high-Q silicon oscillator.[9] By measurement of the resonant frequency and dissipation of the oscillator, the bulk modulus and dissipation in the vortex array can be determined. The oscillator was driven self-resonantly with use of a phase-locked loop.[9] The oscillators had a Q of 2×10^5 at 4.2 K, a frequency of 3 kHz, and a fractional frequency stability of 10^{-8}. The simplest beam-bending mode of the oscillator was

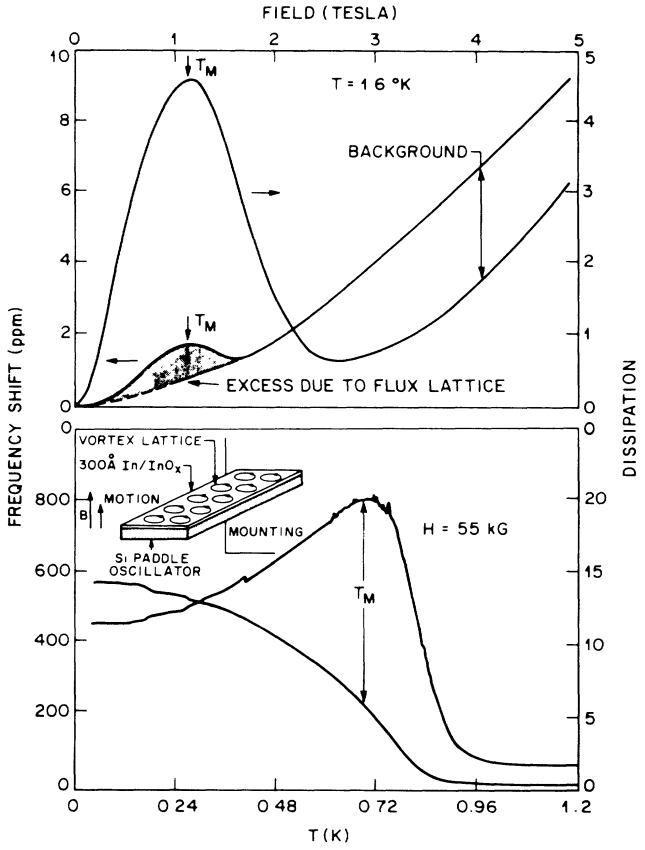

FIG. 1. Bottom: Temperature dependence at fixed magnetic field, or density of vortices. The vortex lattice melts at T_M. Inset: A schematic view of the experiment. Top: At fixed temperature, the vortex lines form a solid at low density and melt as the density is increased. The dissipation and frequency shift scale as H^2 both below and above melting. The melting point is identified as the peak in attenuation.

used. The direction of the motion was parallel to the applied field. To avoid nonlinear effects, a typical amplitude of motion used was 10 nm.

The In/InO_x films were deposited directly onto the oscillator by reactive ion-beam sputter deposition in a low-pressure oxygen environment. The films produced by this technique have been shown to be reproducible and homogeneous.[10] For these experiments, films which were smooth with a predominantly amorphous microstructure were used. Films were also deposited onto a piece of silicon from the same wafer for transport measurements. The resistive transition in zero field was quite sharp, 0.1 K, indicating uniform films. The mean-field transition temperature T_c was estimated from a 40% criterion, rather than a detailed fit to the Aslamazov-Larkin theory.[11] The magnetoresistance of the films was used to determine the upper critical field H_{c2} and the zero-field, vortex-antivortex KT transition temperature, T_{KT}.[12] For the values of $R_\square$ where melting was observed, T_{KT} was within 0.2 K of T_c. The film parameters for the samples studied in these experiments are shown in Table I.

The basic result of the oscillator experiment is shown in Fig. 1. With a uniform magnetic field applied perpendicular to the sample, an array of quantized vortex lines is present. For typical fields, 10 kG, the average spacing is 70 nm. Because the two-dimensional penetration depth, $\Lambda(T)=\lambda^2(T)/d$ where λ is the bulk penetration depth and d is the thickness of the film, is several millimeters, the vortices are strongly overlapping magnetically. However, since the average intervortex spacing $(H/\Phi_0)^{1/2}\gg\xi$ the vortex cores are still well separated. Φ_0 is the superconducting flux quantum and ξ is the coherence length.

When the vortex lattice is in the low-temperature solid phase, a simple physical picture for the oscillator response is possible. The vortex lattice will be collectively pinned, so that the vortices move with the film. In the bending-beam mode, the average vortex spacing, a_0, will oscillate as $\Delta a_0/a_0 \propto A\delta x\, e^{i\omega t}$ where A is the amplitude of oscillation, δ is the thickness of the oscillator, and x is the distance from the suspension point. This density modulation gives a coupling to longitudinal sound in the vortex array at the measurement frequency ω. In two dimensions, the elastic modulus for longitudinal sound is $B+\mu$ where $B\sim H^2$ is the bulk modulus and $\mu\sim H$ is the shear modulus. As a result of the long-range interaction between vortices $B\gg\mu$, and the shear contribution of the vortex array can be neglected.

TABLE I. Parameters for all the films studied.

d (Å)	$R_\square$ (Ω)	T_{c0} (K)	T_{KT} (K)	T_M (K)	A_1
400	313	3.23	3.04	2.24	0.546
500	367	3.00	2.79	2.00	0.483
300	572	2.84	2.58	1.85	0.516
200	904	3.08	2.80		
100	1728	3.22	2.85		

This coupling to longitudinal sound in the vortex array will depend on the relaxation rate of the flux lattice. Since the Hall angle is known to be small,[13] the response of the vortices is purely dissipative. For $T\ll T_M$ there will be a well-formed flux lattice which will remain collectively pinned even in the presence of weak disorder. This will make the relaxation rate for compression of the flux lattice, τ, very long, so that in this regime $\omega\tau\gg 1$ and the vortices will move with the underlying film. Thus an elastic modulus appropriate to longitudinal sound in the vortex lattice will be contributed to the elastic response of the oscillator. For $T\gg T_M$, thermal fluctuations will dominate the motion of the vortices. In this limit, the vortex fluid will relax rapidly ($\omega\tau\ll 1$) and the vortices will not contribute to the elastic response of the film. Near T_M, the compressional relaxation rate will be strongly temperature dependent and a crossover between the two regimes will occur. The peak in attenuation will occur for $\omega\tau\sim 1$, which is the experimentally defined melting temperature.

In the top half of Fig. 1, the dynamic response of the vortex array is examined at fixed temperature by sweeping of magnetic field, or vortex density. At low density, the vortices form a solid. In the solid phase, there is an additional stiffness and dissipation. Both these effects are proportional to H^2. As the solid melts with increasing density, the frequency shift and dissipation decrease. The shaded region in Fig. 1 represents the additional frequency shift due to the flux lattice. The maximum dissipation is identified as the density at which melting occurs. The melting may also be explored at fixed density as a function of temperature, as shown in the lower section of Fig. 1. The excess dissipation which is seen well below the transition temperature has also been observed in helium films,[14] and is associated with internal friction in the vortex solid. The melting temperature is again identified as the maximum in dissipation. The resulting phase diagram is consistent with that given by the field sweeps. In fact, if the curves in the top half of Fig. 1 are divided by the density dependence, H^2, the resulting picture is similar to that seen at fixed density.

If the sample is aligned parallel to the field so that no vortex lattice is present, there are no sharp features in the oscillator response such as those associated with melting. A small frequency shift and dissipation, both proportional to H^2, are still seen. These effects were also seen in an oscillator which had no superconducting film, and are associated with eddy currents in the gold film. This term is identified as the background in Fig. 1.

These data may be combined with the transport data to generate a phase diagram as shown in Fig. 2 for the 313-Ω/□ sample. The results for other samples are qualitatively similar, but the melting line is shifted to lower temperatures as the normal-state sheet resistance is in-

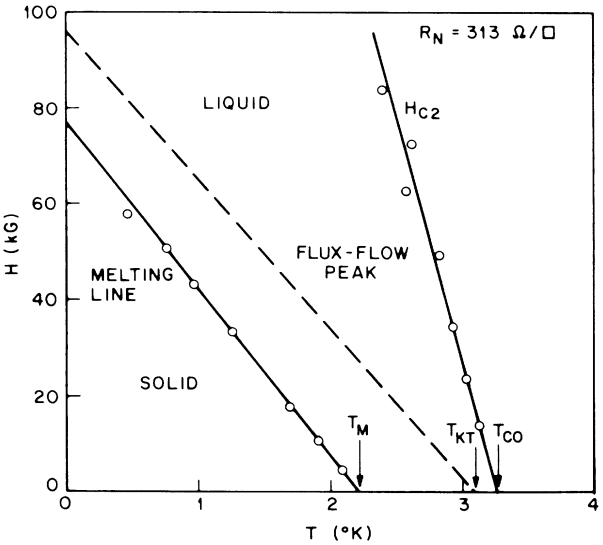

FIG. 2. H_{c2} is obtained from magnetoresistance. Together with the melting data from the oscillator, this is used to generate a phase diagram. Nonlinear I-V curves were used to determine the location of the peak in the volume pinning force.

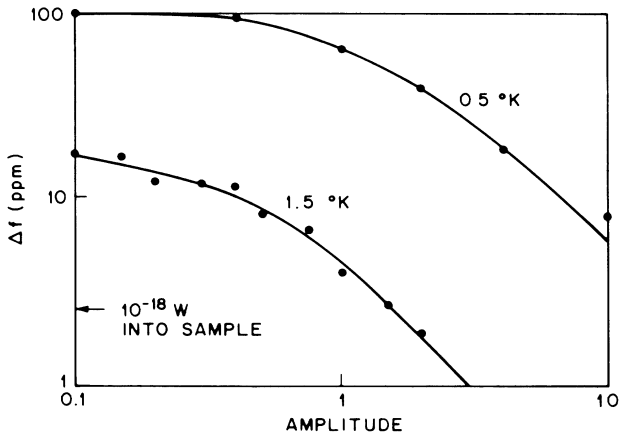

FIG. 3. As the oscillation amplitude is increased, the frequency shift on melting is reduced. The critical velocity increases as the temperature is lowered.

creased, although its slope remains nearly unchanged. The parameters for the three samples in which melting was observed are included in Table I. For normal-state sheet resistances in excess of 900 Ω/□, there was no evidence of solidification, down to 0.3 K, a factor of 4 below the expected melting temperature.

In order to understand the role of pinning in this experiment, I-V curves were measured on the transport samples. In a 400×100-μm^2 sample, the current required to induce 1 μV was defined as the critical current, I_c. The volume pinning force $F_p \propto HI_c$ showed a peak at low fields. The location of this peak is also sketched in Fig. 2. The data were obtained on a sample of higher $R_\square$, so that a larger region below T_c could be explored with our magnet. The data were found to obey the relation $H_{FF}=0.31H_{c2}$. The zero-field intercept was T_{KT}. The dashed line in Fig. 2 is given by this parametrization. Such peaks have been associated with collective pinning phenomena in the vortex array, for samples which showed a peak at high fields.[15] The melting phenomena which we are investigating is clearly distinct from collective pinning. In fact, the 1.3-kΩ/□ sample on which the flux-flow data were taken showed no melting transition.

The effect of increasing the amplitude of motion of the oscillator is shown in Fig. 3, where the frequency shift on melting is shown as a function of oscillation amplitude. For calibration, at an amplitude of 0.1 μm, about 10^{-16} W is dissipated into the 1-cm^2 sample. The critical amplitude increases somewhat as the temperature is reduced. We believe that this is evidence for motionally induced melting of the vortex lattice. A shift in the density at which melting occurs was not observed with increasing amplitude.

The phase diagram has been investigated theoretically[5] for $T_M \ll T_c$. In the intermediate-field regime $\Lambda^2 \gg H/\Phi_0 \gg \xi^2$ relevant to these experiments, the calculated T_M is independent of magnetic field, in contrast to our results. The next-order correction, H/H_{c2}, will suppress melting at high fields in better qualitative agreement with the experiment.[8] At $T=0$, the calculated melting line approaches H_{c2} as $(H-H_{c2})^2$ in the limit of no disorder. We find no departure from the linear slope of the melting line down to 50 mK, our lowest temperature where $H_{c2}\simeq300$ kG and melting occurs at 80 kG. In the presence of disorder, a perfect lattice is no longer expected. As a result of even small amounts of pinning, the quasi long-range order of the flux lattice is destroyed, and there is no sharp melting transition. However, for weak disorder, there will still be solid order out to long distances and pinning will not be too significant. As H approaches H_{c2} pinning becomes more important.[5] The transition width, which is found to be proportional to field, is further evidence for the increasing importance of disorder in high fields. The high-field phase at low temperatures has been conjectured to be an amorphous solid rather than a liquid.[8] The amorphous solid phase may also be responsible for the transition widths. In fact, for samples with normal-state sheet resistances greater than 900 Ω/□, the disorder is sufficiently great to inhibit the growth of a crystalline solid for all temperatures and densities.

In the limit of low normal-state sheet resistance, $R_\square/R_c \ll 1$, the calculated melting temperature with standard dirty-limit expressions is $T_c/T_M=(1+3.8R_\square/A_1R_c)$. $R_c=4.12$ kΩ/□ is a characteristic resistance near which superconductivity vanishes. This result can be compared to the zero-field extrapolation of the measured melting line to give the values of A_1 in Table I. For a KT-type transition, it is estimated[5] that 0.4

$< A_1 < 0.75$. The measured value $A_1 \simeq 0.5$ falls within this range. Because this experiment does not probe the shear modulus, the validity of the KT universal jump criterion $\mu(T_M)a_0^2/k_B T_M = 4\pi$, where a_0 is the lattice constant, cannot be determined.

The remarkable stiffness of the vortex solid is demonstrated by this experiment. Using the ratio of film thickness to that of the oscillator, 10^{-4}, we may estimate the magnitude of the elastic modulus of the vortex solid. At low temperatures, in an 80-kG applied field, the frequency shift on melting is of order 5×10^{-4}. This implies that the elastic modulus of the vortex lattice is nearly 10 times that of silicon at the lowest temperatures. The bulk modulus may be obtained from the total interaction energy of the vortex array,

$$[\Phi_0^2/8\pi^2\Lambda(T)]\int n(r)\ln(r-r')n(r')d^2r\,d^2r'.$$

The integral is cut off either by the finite system size or by $\Lambda(T)$. Either length scale is approximately 1 cm. Since the density is given by $n = H/\Phi_0$, this gives the observed H^2 dependence. The estimated modulus is 100 kbar for a lattice constant of 50 nm ($H = 20$ kG) which is similar to bulk silicon and in rough agreement with experiment.

In conclusion, we have used a novel high-Q mechanical-oscillator technique to study flux-lattice melting in amorphous In/InO_x thin-film superconductors. The phase diagram has been explored for a variety of normal-state resistances. A theory based on KT melting can qualitatively describe the data, but differs in its quantitative features. The theory contains one parameter which may be used to fit the zero-field extrapolation of the melting temperature for the different normal-state sheet resistances. However, the theory predicts a melting temperature independent of magnetic field. Our result, the melting temperature being reduced linearly with field, may be due to either the required H/H_{c2} corrections[8] to the theory or the increasing role of pinning at high fields. The observed bulk modulus of the vortex solid exceeds that of bulk silicon below 0.1 K in 80 kG fields, which can be understood in terms of the long-range interactions between vortices.

We would especially like to thank D. S. Fisher for numerous discussions and continuing interest in this experiment. We would also like to thank A. Millis for many helpful discussions and R. H. Eick for technical assistance.

[1]A. A. Abrikosov, Zh. Eksp. Teor. Fiz. **32**, 1442 (1957) [Sov. Phys. JETP **5**, 1174 (1957)].

[2]H. Trauble and U. Essman, J. Appl. Phys. **25**, 273 (1968).

[3]D. Cribier, B. Jacrot, L. M. Rao, and B. Farnoux, Phys. Lett. **9**, 106 (1964).

[4]E. Conen and A. Schmid, J. Low Temp. Phys. **17**, 331 (1974); A. L. Fetter and P. C. Hohenberg, Phys. Rev. **159**, 330 (1967).

[5]D. S. Fisher, Phys. Rev. B **22**, 1190 (1980).

[6]B. A. Huberman and S. Doniach, Phys. Rev. Lett. **43**, 950 (1979).

[7]A. T. Fiory and A. F. Hebard, Phys. Rev. B **25**, 2073 (1982).

[8]D. S. Fisher, private communication.

[9]R. N. Kleiman, G. K. Kaminsky, J. D. Reppy, R. Pindak, and D. J. Bishop, Rev. Sci. Instrum. **56**, 2088 (1985).

[10]A. F. Hebard and S. Nakahara, Appl. Phys. Lett. **41**, 1130 (1982).

[11]M. A. Paalanen and A. F. Hebard, Appl. Phys. Lett. **45**, 794 (1984).

[12]A. F. Hebard and M. A. Paalanen, Phys. Rev. Lett. **54**, 2155 (1985).

[13]Y. B. Kim and M. J. Stephen, in *Superconductivity*, edited by R. D. Parks (Dekker, New York, 1969), Vol. 2, pp. 1107–1167.

[14]D. J. Bishop and J. D. Reppy, Phys. Rev. Lett. **40**, 1727 (1978), and Phys. Rev. B **22**, 5171 (1980).

[15]P. H. Kes and C. C. Tsui, Phys. Rev. B **28**, 5126 (1983).

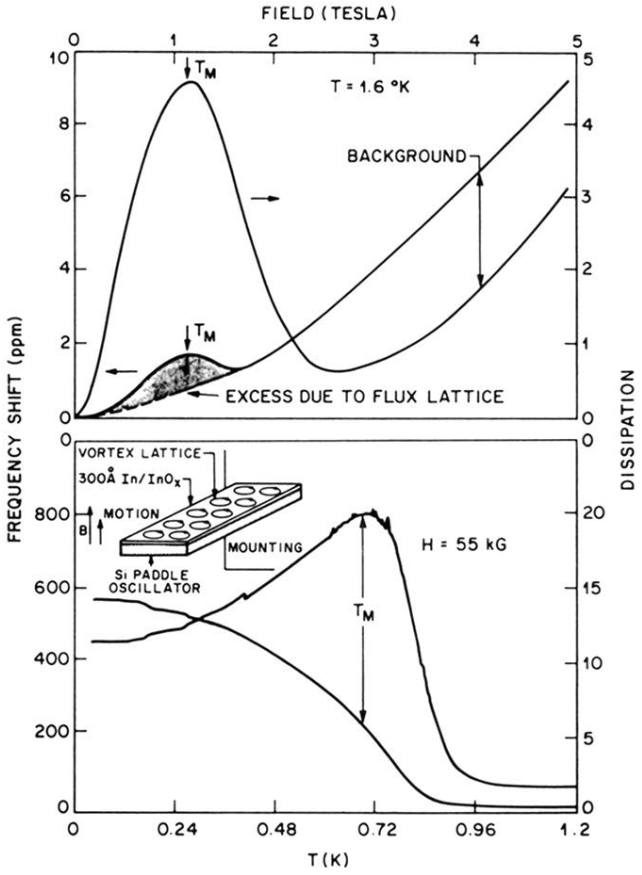

FIG. 1. Bottom: Temperature dependence at fixed magnetic field, or density of vortices. The vortex lattice melts at T_M. Inset: A schematic view of the experiment. Top: At fixed temperature, the vortex lines form a solid at low density and melt as the density is increased. The dissipation and frequency shift scale as H^2 both below and above melting. The melting point is identified as the peak in attenuation.